Article

Potential of AlN Nanostructures as Hydrogen Storage Materials

Qian Wang, Qiang Sun, Puru Jena, and Yoshiyuki Kawazoe

ACS Nano, **2009**, 3 (3), 621-626• Publication Date (Web): 03 March 2009

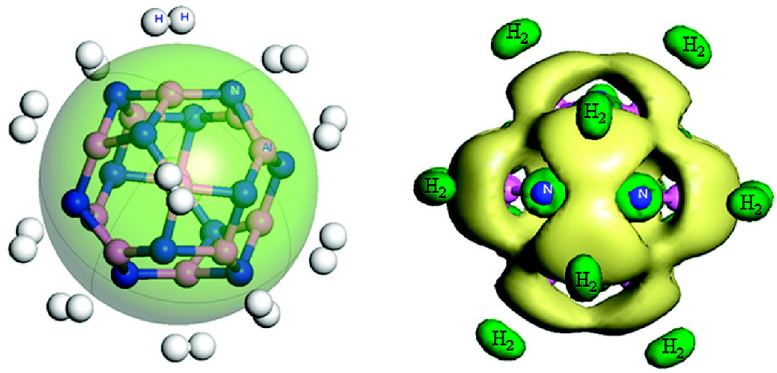

More About This Article

Additional resources and features associated with this article are available within the HTML version:

- Supporting Information
- Access to high resolution figures
- Links to articles and content related to this article
- Copyright permission to reproduce figures and/or text from this article

View the Full Text HTML

Potential of AlN Nanostructures as Hydrogen Storage Materials

Qian Wang,[†] Qiang Sun,[‡,†,*] Puru Jena,[†] and Yoshiyuki Kawazoe[§]

[†]Department of Physics, Virginia Commonwealth University, Richmond, Virginia 23284, [‡]Department of Advanced Materials and Nanotechnology and Center for Applied Physics and Technology, Peking University, Beijing 100871, China, and [§]Institute for Materials Research, Tohoku University, Sendai 980-8577, Japan

ABSTRACT The capability of AlN nanostructures (nanocages, nanocones, nanotubes, and nanowires) to store hydrogen has been studied using gradient-corrected density functional theory. In contrast to bulk AlN, which has the wurtzite structure and four-fold coordination, the Al sites in AlN nanostructures are unsaturated and have two- and three-fold coordination. Each Al atom is capable of binding one H_2 molecule in quasi-molecular form, leading to 4.7 wt % hydrogen, irrespective of the topology of the nanostructures. With the exception of AlN nanotubes, energetics does not support the adsorption of additional hydrogen. The binding energies of hydrogen to these unsaturated metal sites lie in the range of 0.1−0.2 eV/H_2 and are ideal for applications under ambient thermodynamic conditions. Furthermore, these materials do not suffer from the clustering problem that often plagues metal-coated carbon nanostructures.

KEYWORDS: hydrogen storage · nanostructure with exposed metal sites · cage · tube · cone · wire

Hydrogen, the third most abundant element on earth, has the potential to meet the energy needs of the mobile industry. However, its economical use as an alternate energy has substantial difficulties to overcome. Among these, the most difficult challenge is to find materials that can store hydrogen with large gravimetric and volumetric density and operate under ambient thermodynamic conditions. The Department of Energy's system target for the ideal hydrogen storage material is that the gravimetric density of hydrogen should reach 6 wt % by 2010. In addition, the storage materials should be able to reversibly adsorb/desorb H_2 in the temperature range of −20 to 50 °C and under moderate pressures (max. 100 atm). The first requirement limits the choice of storage materials to be composed of elements lighter than Al, while the latter requires hydrogen binding energies to be between physisorption and chemisorption energies.

Recently Bhatia and Myers[1] have studied the optimum thermodynamic conditions for hydrogen adsorption by employing the Langmuir equation and derived relationships between the operating pressure of a storage tank and the enthalpy of adsorption required for storage near room temperature. They have found that the average optimal adsorption enthalpy should be 15.1 kJ /mol if operated between 1.5 and 30 bar at 298 K. When the pressure is increased to 100 bar, the optimal value becomes 13.6 kJ/mol. Therefore, the optimal adsorption energy for H_2 should be in the range of 0.1−0.2 eV/H_2. Unfortunately, the above two requirements are difficult to satisfy simultaneously. The bonding of hydrogen in light elements is either too strong, as in light metal hydrides and organic molecules, or too weak, when interacting with graphite and carbon and BN fullerenes and nanotubes.[2−5] For example, in MgH_2, the storage capacity of hydrogen is as high as 7.6 wt %, but high temperature (~573 K) is needed to release H_2 as the hydride bond is very strong (~75 kJ/mol), and in many cases, such processes are often irreversible.[6,7] Aluminum hydride (AlH_3), although it contains 10 wt % H, has to be heated over 100 °C to release hydrogen.[8]

To circumvent this problem, a new form of hydrogen bonding, which is intermediate between physisorption and chemisorption, has attracted considerable attention in recent years. Following the Kubas mechanism,[9] it was shown[10,11] that transition-metal atoms supported on carbon fullerenes and nanotubes can bind hydrogen in quasi-molecular form, where the H−H bond is slightly stretched and binding energies lie in the range of 0.5−0.8 eV/H_2. However, later studies[12] showed that these metal atoms have a tendency to cluster and hence undermine their hydrogen storage capability. A different mechanism, proposed by Rao and Jena more than a decade ago,[13] had shown that a positively charged metal atom can also bind

*Address correspondence to sunqiang@pku.edu.cn.

Received for review November 30, 2008 and accepted February 23, 2009.

Published online March 3, 2009.
10.1021/nn800815e CCC: $40.75

to a large amount of hydrogen in quasi-molecular form due to the charge polarization mechanism. In applying this mechanism to real materials, one has to keep in mind that the metal atom has to remain in a positively charged state. Note that in molecules, nanostructures, and solids no free ions exist. In ionic systems, however, an atom, due to charge transfer, can remain in a positive charge state, which is counter balanced by the negative charge on a different site. This mechanism, when applied to Li-coated C_{60}, permitted $Li_{12}C_{60}$ to adsorb up to 13 wt % hydrogen, but the binding energies were too low for room-temperature applications.[14] The challenge, therefore, has been to find systems where clustering of metal atoms can be prevented without compromising the binding energy of hydrogen.

Recent efforts have focused on exposed light metal sites such as Al^{3+}, Mg^{2+}, and Li^{+} in light material substrate.[15−17] Three strategies have been developed to introduce the exposed metal sites: (1) removing the metal-bound volatile species, which typically function as terminal ligands; (2) incorporating metal species; and (3) impregnating materials with excess metal cations. Theoretically, it has been found recently[18] that a free Al^{3+} ion has a strong ability to interact with H_2 molecules, and the interaction energy can reach 354.13 kJ/mol. When ligand molecules such as CN and CO are attached to the Al^{3+} ion, the interaction energy with H_2 is reduced. This implies that when Al ions are embedded in some appropriate matrices, the adsorption energy of hydrogen molecules can be tuned. Thus, the question arises: How can one introduce Al ions in a natural way to materials and make the system have desirable hydrogen storage properties? It will be ideal if these metal centers form the intrinsic backbone of the storage material so that their clustering will not be an issue to deal with.

This study provides a solution. The answer lies in the choice of AlN nanostructures such as nanocages, nanohorns, nanotubes, and nanowires. Bulk AlN has wurtzite structure, where each Al ion is four-fold coordinated. It is a wide band gap semiconductor with a band gap of 6.2 eV and exhibits good dielectric properties, high thermal conductivity, and low thermal expansion coefficient. It also has potentials for application in deep ultraviolet optoelectronics and spintronics.[19] We are not aware of any studies where bulk AlN has been considered as a hydrogen storage material. Unlike carbon, which forms a planar graphite structure as its ground state, AlN does not form a layered structure. However, AlN, similar to that of C, exists in the form of nanocones, nanotubes, and nanowires, although the electronic structure of AlN nanocages is very different from that of C_{60}, where three-fold C atoms are stabilized by a rather strong π bonding, which is nearly not the case for Al. AlN nanostructures have been successfully synthesized from the nonlayered structure.[20−26] On the surface of these nanostructures, Al ion is two- or three-fold coordinated. When going from the four-fold coordinated bulk phase to the two- or three-fold coordinated nanostructured surfaces, unsaturated Al sites are naturally introduced. We show that these sites, which are an integral part of the nanostructures, carry a positive charge and provide the desirable adsorption sites for H_2 molecules.

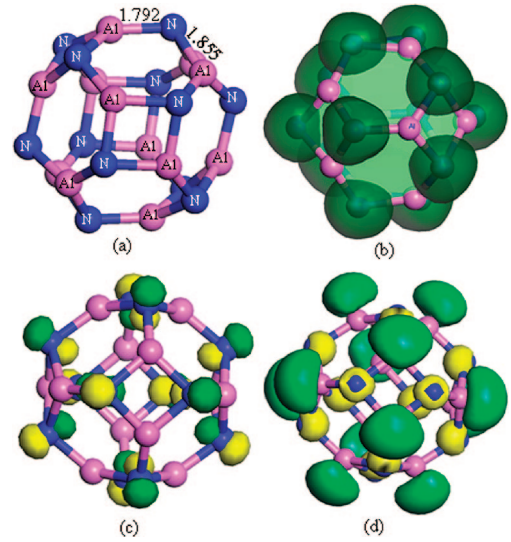

Figure 1. (a) Geometry, (b) charge density difference, (c) HOMO, and (d) LUMO of the $Al_{12}N_{12}$ cage.

We begin our studies with calculations of the electronic properties and adsorption of hydrogen molecules in the $Al_{12}N_{12}$ cage. The geometry of this cage has been found to be composed of six four-membered rings having T_h symmetry.[27−29] There are two nonequivalent Al−N bonds: Al−N bond in the four-membered ring has a length of 1.855 Å, while the Al−N bond between the four-membered rings has a length of 1.792 Å, as shown in Figure 1a. Because of the large difference in electronegativity between Al and N, ionic bonding is predominant in the $Al_{12}N_{12}$ cage. This can be seen from the charge difference (with respect to free atoms) plotted in Figure 1b, where N sites receive electrons from Al sites, resulting in positively charged Al ions. A charge analysis based on the Wigner−Seitz cell method for charge partitioning indicates that the charge state of the Al ion is close to +1. The highest occupied molecular orbital (HOMO) of the cage is three-fold degenerate with T_u symmetry and mainly localized on N sites (see Figure 1c), while the lowest unoccupied molecular orbital (LUMO) is nondegenerate with A_g symmetry and is predominantly localized on Al sites (see Figure 1d).

The positively charged Al ions on the cage surface become the available sites for adsorption of H_2 molecules. As a matter of fact, we found that when a H_2 molecule is introduced on the cage surface the H_2 molecule is adsorbed on top of the Al site at a distance of 2.179 Å with a binding energy of 0.212 eV/H_2 (see Figure 2a). The polarization of the H_2 molecule caused by the charge on the Al ion leads to an elongation of the

H_2 bond length from 0.740 Å of its equilibrium value in the free state to 0.762 Å. As each Al site on the cage surface is decorated with one H_2 molecule, all of the geometrical parameters of the cage remain almost unchanged (Figure 2b). The average adsorption energy decreases slightly to 0.190 eV/H_2. Note that the required energy window for storage under ambient conditions is about 0.2 eV/H_2.[1] In addition, the corresponding gravimetric density of hydrogen, namely, 4.7 wt %, approaches the 2010 DOE target of 6 wt %. It is interesting to note that, after H_2 adsorption, the frontier orbital of the complex is contributed primarily by the Al sites and H_2 molecules (see Figure 2c). The Al atoms are locked in their original sites, and no clustering is formed. Thus, our calculated results show that the AlN nanocage possesses the desirable properties for hydrogen storage. A recent study indicated that $Al_{12}N_{12}$ can be used as building blocks for nanomaterials.[29]

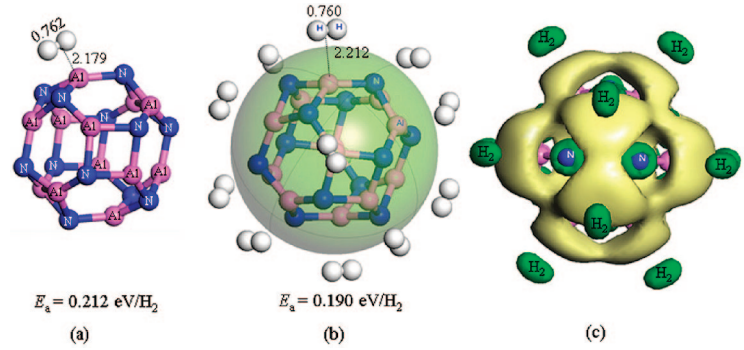

Figure 2. (a) Single H_2 and (b) 12 H_2 molecules adsorbed on the $Al_{12}N_{12}$ cage surface. (c) LUMO of the $12H_2-Al_{12}N_{12}$ cage.

There are two main mechanisms involved in adsorption of H_2 molecules on Al ions: charge-induced interaction (electrostatic effect) and orbital interactions. As H_2 molecules approach the positively charged Al ions, the charge on Al ions polarizes the electron clouds in H_2, inducing electrostatic interactions. However, we found that the changes of adsorption energy, E_a, with the distance, R, from the Al ion do not quite scale as $\sim 1/R$,[3] suggesting that other factors might also be involved in hydrogen bonding. In fact, the charge analysis indicates that, when H_2 molecules are adsorbed, each H_2 molecule carries a charge of $+0.05e$. This is due to low lying unoccupied valence orbitals available in Al ions, which allows mixing with the σ bonding orbital of H_2, resulting in the donation of the σ electrons into the vacant orbitals of Al ions. The H_2 adsorption is accordingly improved.

We attempted to attach a second H_2 molecule to each of the Al ions in the $Al_{12}N_{12}$ cage and optimized the structure. However, the H_2 molecules were found to move away from the cage to a distance of 3.322 Å. Correspondingly, the average adsorption energy decreases to 0.072 eV/H_2. This is in contrast to what was observed for a Li^+ ion.[14] The reason could be that the Al^+ ion is much larger than the Li^+ ion and hence its electrons interact with the antibonding orbitals of H_2 as noted above.

We next extended the idea of using the unsaturated charged metal sites for hydrogen storage to the AlN nanocone. We construct a cone with the disclination angle of 240° consisting of $Al_{36}N_{36}$ to model AlN nanocones synthesized in experiments.[20−23] The base diameter is 11.50 Å (see Figure 3a). The edge atoms in the $Al_{36}N_{36}$ cone are terminated with 12 H atoms (see Figure 3a). The dynamic stability of geometry is conformed by frequency calculations. Unlike the $Al_{12}N_{12}$ cage where all the Al or N atoms are equivalent, the symmetry of the AlN nanocone is low. We have found that the frontier orbitals are mainly located in the tip area (see Figure 3b), suggesting applications of nanocones in field emission. Therefore, the adsorption of hydrogen molecules in the nanocone is expected to be different for the different Al sites. We found the adsorption energy to be 0.215 eV/H_2 when a H_2 molecule is introduced at the uppermost Al site (see Figure 4a). The equilibrium distance between the Al site and the H_2 is 2.115 Å, and the bond length of H−H becomes 0.769 Å. However, when a H_2 molecule is introduced at the nearest neighbor site to the uppermost Al atom, as shown in Figure 4b, the adsorption energy reduces slightly to 0.195 eV/H_2 and becomes 0.113 eV/H_2 when the adsorption site is nearer to the base of the cone (see Figure 4c). Thus, the adsorption of H_2 molecules on the AlN nanocone is anisotropic and driven by the morphology of the nanocone.

We have also studied the effect of dimensionality of AlN nanostructures on their potential for storing hydrogen by considering nanotubes and nanowires. We generated an AlN single-wall nanotube from an ($8 \times 8 \times 2$) AlN supercell having wurtzite structure by removing the Al and N atoms from the inner and the outer part the two circles in Figure 5a along the [0001] direction. The supercell used to model the nanotube, thus,

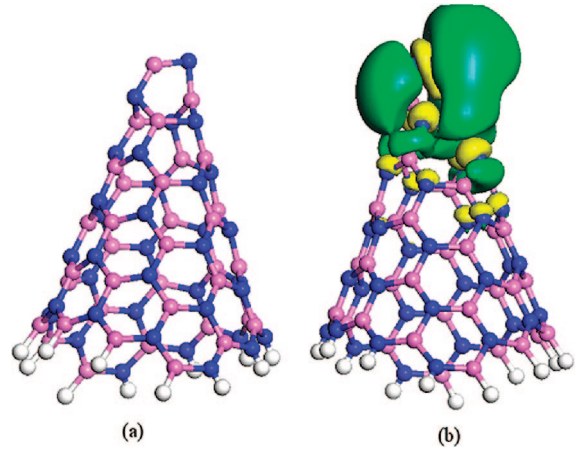

Figure 3. (a) Geometry and (b) HOMO of AlN nanocone. The magenta spheres represent Al atoms, the blue spheres represent N atoms, and the white spheres represent H atoms.

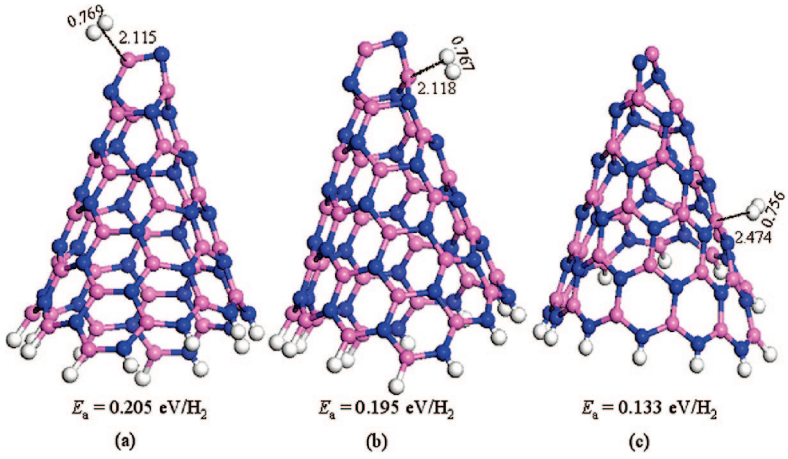

Figure 4. Adsorption of a single hydrogen molecule on different Al sites in the AlN nanocone.

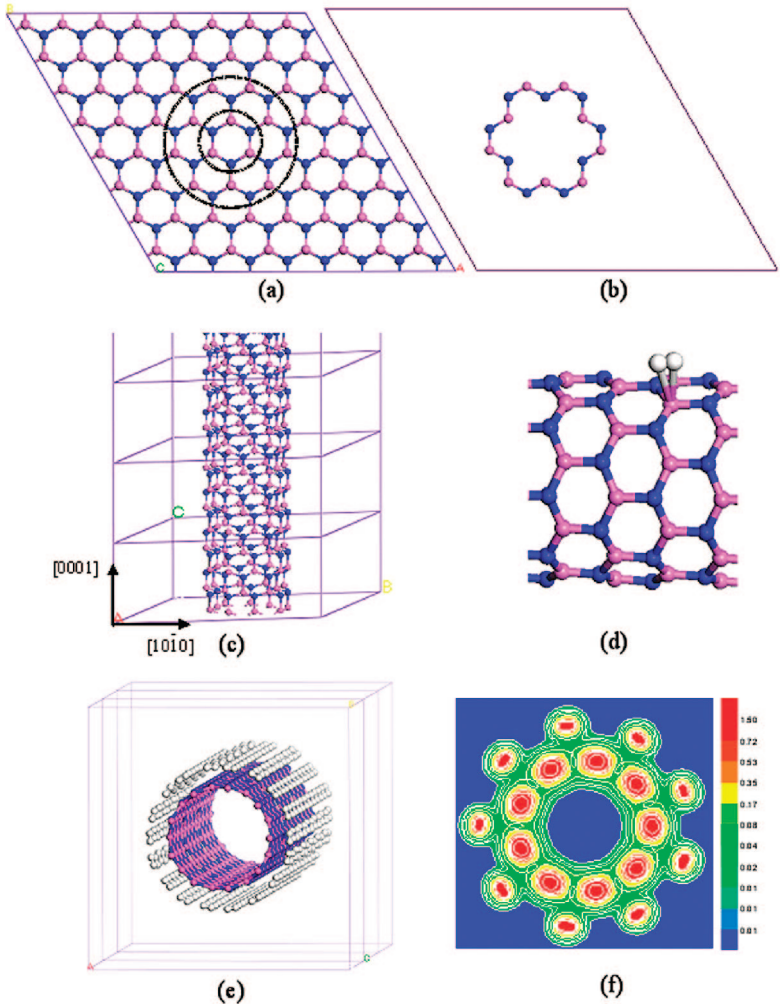

Figure 5. (a) Top view of an 8 × 8 × 2 AlN supercell having wurtzite structure. (b) Top view of the unrelaxed AlN nanotube. (c) Side view of the optimized AlN nanotube extending to infinity along the [0001] direction. (d) Adsorption of a single hydrogen molecule at the Al site on the nanotube. (e) Adsorption of hydrogen molecules at each Al site of the nanotube, and (f) charge density distribution of H_2 molecules on the nanotube supercell. The magenta spheres represent Al atoms, the blue spheres represent N atoms, and the white spheres are H atoms.

has a total of 36 formula units of AlN. We used a vacuum space of ~15.0 Å along the [10$\bar{1}$0] and [01$\bar{1}$0] directions. The supercell has a polygon periphery with diameters of 9.525 Å for the outer shell and 7.211 Å for the inner shell when viewed from the central tube axis along the [0001] direction (see Figure 5b). It extends to infinity along the [0001] direction through the repetition of the periodic supercell (see Figure 5c). After full optimization, the cross section of the tube no longer exhibits the zigzag shape characteristic of the bulk wurtzite structure, and the tube has a diameter of 9.463 Å, similar to that of carbon (9,0) single-wall nanotube.

To study the adsorption of hydrogen molecules on the nanotube, we first introduce a single H_2 on an Al site on the outer tube surface, as shown in Figure 5d. The corresponding adsorption energy is found to be 0.157 eV/H_2. The distance between the H_2 and the Al ion is 2.524 Å, and that between H−H is 0.753 Å. When one H_2 molecule was attached to each Al site on the tube surface (see Figure 5e), the absorption energy and the bond length of H_2 remained essentially unchanged, namely, 0.152 eV/H_2 and 0.752 Å, respectively. The H_2 molecules are found to be 2.620 Å away from the tube surface. In Figure 5f, we plot the charge distribution, which shows the orbital mixing interaction between AlN nanotube and H_2 molecules as discussed above. To see if hydrogen can also be stored inside the nanotube, we introduced 12 H_2 molecules in the interior of the tube and reoptimized the structure. Note that adding more H_2 molecules inside the tube would encounter steric hindrance. The resulting geometry and the charge density distribution are plotted in panels a and b of Figure 6, respectively. The H_2 molecules inside the nanotube lie at a distance of 2.890 Å from the Al site, while those on the outer surface moved to a distance of 2.696 Å. As a result, the average adsorption energy reduces to 0.101 eV/H_2. Although adding the 12 H_2 molecules inside the nanotube can raise the hydrogen gravimetric density to 6.15 wt %, the reduction in the binding energy may be detrimental for application under ambient conditions. In addition, an energy barrier may prevent H_2 molecules from entering the nanotube.[5]

We further studied hydrogen adsorption on AlN nanowires. For this, we created the thinnest possible AlN nanowire by following the same procedure as described for the nanotube construction, but by using a (5 × 5 × 2) AlN bulk supercell. The nanowire has infinite length along the [0001] direction, and its cross section consists of three AlN pairs (see Figure 7a). When one H_2 molecule is introduced to each Al site of the nano-

wire, the average adsorption energy is found to be 0.192 eV/H_2. The H−H bond length is calculated to be 0.760 Å, and the distance between the H_2 molecules and the corresponding Al atoms in the nanowire is found to be 2.201 Å.

There are several concerns that need to be addressed regarding the feasibility of using AlN nanostructures in practical applications, and we address these in the following: (1) The unsaturated sites in the nanostructures are reactive and can easily bind to unwanted gases such as oxygen. This concern can apply to all metal-decorated nanostructures that are being pursued for hydrogen storage. In real applications, care must, therefore, be taken to shield these structures from unwanted gases. We note that AlN nanostructures in the form of nanocones, nanotubes, and nanowires have been successfully synthesized from the nonlayered structures.[20−26] (2) DFT does not treat weakly bound systems well as it does not take into account dispersion forces. In a recent paper,[30] it has been demonstrated that the adsorption energy of molecules to a substrate is underestimated when dispersion forces are not taken into account. Therefore, the adsorption of H_2 molecules in AlN nanostructures is actually slightly stronger than that we calculated. (3) The calculations are performed at 0 K, while applications are at room temperatures. As mentioned earlier, Bhatia and Myers[1] have shown that adsorption energy in the range of 0.1−0.2 eV/H_2 is required for storage near room temperature. Our results are consistent with these values and thus suggest that AlN nanostructures are appropriate for hydrogen storage under ambient conditions.

In summary, we have shown that AlN nanostructures, such as nanocages, nanocones, nanotubes, and nanowires, can bind hydrogen in quasi-molecular form with binding energies of about 0.200 eV/H_2. The advantage of using AlN nanostructures is that no additional metal doping is necessary and hence any difficulty with the clustering of deposited metal atoms is avoided. The Al sites, due to difference in electronegativities between Al and N, remain positively charged and bind hydrogen primarily through a charge polarization mechanism. Each Al−N pair can adsorb one H_2, yielding a gravimetric density of 4.7 wt %, irrespective of the morphology of the nanostructures. Since the Al sites form the intrinsic backbone of the AlN nanosystems, one can avoid complicated methods for producing exposed metal sites such as removing the metal-bound volatile species, incorporating metal species, or impregnating materials with excess metal cations.[15] We hope that the present study will stimulate new experiments.

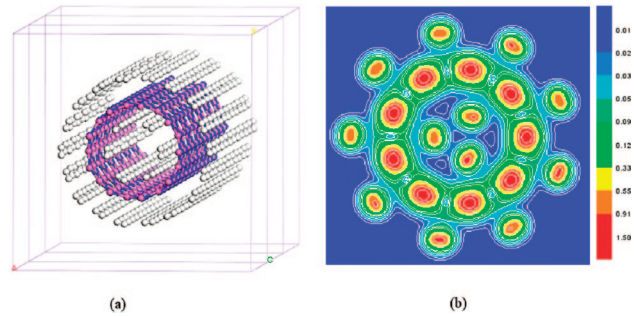

Figure 6. (a) Adsorption of hydrogen molecules at each Al site on the outer surface and at the second next adjacent Al site on the inner surface of the nanotube, and (b) charge density distribution of H_2 molecules on $48H_2-Al_{36}N_{36}$ nanotube supercell.

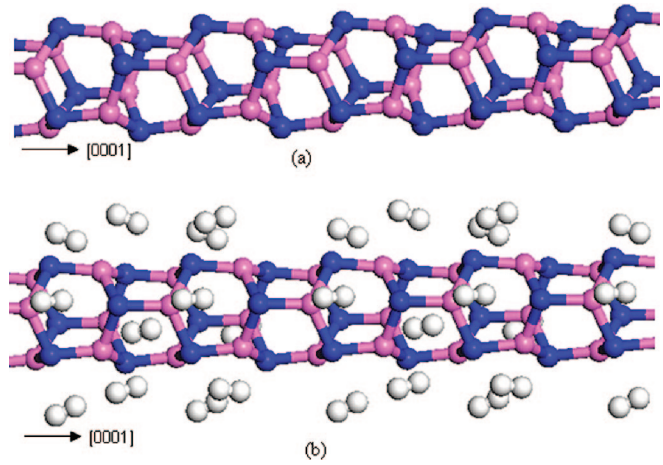

Figure 7. Geometry of an infinite AlN nanowire along the [0001] without (a) and with (b) H_2 molecules attached. The magenta spheres represent Al atoms, the blue spheres represent N atoms, and the white spheres represent H atoms.

COMPUTATIONAL METHODS

The calculations of total energies, forces, and optimization of geometries have been carried out using generalized gradient approximation (GGA)[31] to the density functional theory (DFT) and the projector augmented wave (PAW)[32] method as implemented in the Vienna Ab Initio Simulation Package (VASP).[33] The PW91 potentials[34] with the valence states of $3s^2p^1$ for Al and $2s^2p^3$ for N were used for the GGA functional. We used a supercell approach where the zero-dimensional finite systems (nanocage and nanocone) are surrounded by 15 Å of vacuum space along the *x*, *y*, and *z* directions, and the Γ point is used to represent the Brillouin zone due to the large supercell. For the one-dimensional systems (*i.e.*, nanotube and nanowire) that have infinite length along the [0001] direction, a vacuum space of 15 Å is applied to the [10$\bar{1}$0] and [01$\bar{1}$0] directions, and the periodic condition is maintained in the [0001] direction. The (1 × 1 × 6) and (1 × 1 × 8) Monkhorst−Pack grids[35] are selected, respectively, for the structure optimization and for total energy and charge density calculations. In all of the calculations, the atomic coordinates of all the atoms in the supercells were relaxed without any symmetry constraint by using a conjugate-gradient algorithm. The energy cutoff and the convergence in energy and force were set to 450 eV, 10^{-4} eV, and 1×10^{-3} eV/Å, respectively. The accuracy of our numerical procedure for Al, N, and H has been demonstrated in our previous papers.[5,12,14,19,36]

Acknowledgment. This work is partially supported by grants from the U.S. Department of Energy and the National Natural Science Foundation of China (NSFC-10744006, NSFC-10874007). The authors thank the crew of the Center for Computational Materials Science, the Institute for Materials Research, Tohoku Uni-

versity (Japan), for their continuous support of the HITACH SR11000 supercomputing facility.

REFERENCES AND NOTES

1. Bhatia, S. K.; Myers, A. L. Optimum Conditions for Adsorptive Storage. *Langmuir* **2006**, *22*, 1688–1700.
2. Shiraishi, M.; Takenobu, T.; Ata, M. Gas−Solid Interactions in the Hydrogen/Single-Walled Carbon Nanotube System. *Chem. Phys. Lett.* **2003**, *367*, 633–636.
3. Kajiura, H.; Tsutsui, S.; Kadono, K.; Kakuta, M.; Ata, M.; Murakami, Y. Hydrogen Storage Capacity of Commercially Available Carbon Materials at Room Temperature. *Appl. Phys. Lett.* **2003**, *82*, 1105–1107.
4. Dodziuk, H.; Dolgonos, G. Molecular Modeling Study of Hydrogen Storage in Carbon Nanotubes. *Chem. Phys. Lett.* **2002**, *356*, 79–83.
5. Sun, Q.; Wang, Q.; Jena, P. Storage of Molecular Hydrogen in B−N Cage: Energetics and Thermal Stability. *Nano Lett.* **2005**, *5*, 1273–1277.
6. Fichtner, M. Nanotechnological Aspects in Materials for Hydrogen Storage. *Adv. Eng. Mater.* **2005**, *7*, 443–455.
7. Grochala, W.; Edwards, P. P. Thermal Decomposition of the Non-Interstitial Hydrides for the Storage and Production of Hydrogen. *Chem. Rev.* **2004**, *104*, 1283–1315.
8. Alefeld, G.; Völkl, J. *Hydrogen in Metals II. Topics in Applied Physics*; Springer Press: Berlin, 1978; Vol. 29, pp 15−120.
9. Kubas, G. J. Molecular Hydrogen Complexes: Coordination of a Sigma-Bond to Transition-Metals. *Acc. Chem. Res.* **1988**, *21*, 120–128.
10. Zhao, Y. F.; Kim, Y. H.; Dillon, A. C.; Heben, J. M.; Zhang, S. B. Hydrogen Storage in Novel Organometallic Buckyballs. *Phys. Rev. Lett.* **2005**, *94*, 155504-1–155504-4.
11. Yildirim, T.; Ciraci, S. Titanium-Decorated Carbon Nanotubes as a Potential High-Capacity Hydrogen Storage Medium. *Phys. Rev. Lett.* **2005**, *94*, 175501–175504.
12. Sun, Q.; Wang, Q.; Jena, P.; Kawazoe, Y. Clustering of Ti on a C-60 Surface and Its Effect on Hydrogen Storage. *J. Am. Chem. Soc.* **2005**, *127*, 14582–14583.
13. Rao, B. K.; Jena, P. Hydrogen Uptake by an Alkali-Metal Ion. *Europhys. Lett.* **1992**, *20*, 307–312.
14. Sun, Q.; Jena, J.; Wang, Q.; Marquez, M. First-Principles Study of Hydrogen Storage on $Li_{12}C_{60}$. *J. Am. Chem. Soc.* **2006**, *128*, 9742–9745.
15. Dinca, M.; Long, J. R. Hydrogen Storage in Microporous Metal-Organic Frameworks with Exposed Metal Sites. *Angew. Chem., Int. Ed.* **2008**, *47*, 6766–6779.
16. Wang, Q.; Sun, Q.; Jena, P.; Kawazoe, Y. Mg-Doped GaN Nanostructures: Energetics, Magnetism, and H_2 Adsorption. *Appl. Phys. Lett.* **2009**, *94*, 013108–013110.
17. Sun, Q.; Wang, Q.; Jena, P. Functionalized Heterofullerenes for Hydrogen Storage. *Appl. Phys. Lett.* **2009**, *94*, 013111–013113.
18. Lochan, R. C.; Head-Gordon, M. Computational Studies of Molecular Hydrogen Binding Affinities: The Role of Dispersion Forces, Electrostatics, and Orbital Interactions. *Phys. Chem. Chem. Phys.* **2006**, *8*, 1357–1370.
19. Wang, Q.; Kandalam, A. K.; Sun, Q.; Jena, P. Ferromagnetism in $Al_{1-x}Cr_xN$ Thin Films by Density Functional Calculations. *Phys. Rev. B* **2006**, *73*, 115411-1–115411-7.
20. Liu, C.; Hu, Z.; Wu, Q.; Wang, X.; Chen, Y.; Sang, H.; Zhu, J.; Deng, S.; Xu, N. Synthesis and Field Emission Properties of Aluminum Nitride Nanocones. *J. Am. Chem. Soc.* **2005**, *127*, 1318–1322.
21. Li, Y. L.; Shi, C. Y.; Li, J. J.; Gu, C. Z. Local Field-Emission Characteristic of Individual AlN Cone Fabricated by Focused Ion-Beam Etching Method. *Appl. Surf. Sci.* **2008**, *254*, 4840–4844.
22. Liu, C.; Hu, Z.; Wu, Q.; Wang, X.; Chen, Y.; Lin, W.; Sang, H.; Deng, S.; Xu, N. Synthesis and Field Emission Properties of Aluminum Nitride Nanocones. *Appl. Surf. Sci.* **2005**, *251*, 220–224.
23. Liu, C.; Hu, Z.; Wu, Q.; Wang, X.; Chen, Y.; Zhu, J. Controllable Synthesis of One-Dimensional Aluminum Nitride Nanostructures through Vapor-Solid Epitaxial Growth. *J. Nanoelectron. Optoelectron.* **2006**, *1*, 114–118.
24. Wu, Q.; Hu, Z.; Wang, X.; Lu, Y.; Chen, X.; Xu, H.; Chen, Y. Synthesis and Characterization of Faceted Hexagonal Aluminum Nitride Nanotubes. *J. Am. Chem. Soc.* **2003**, *125*, 10176–10177.
25. Balasubramanian, C.; Godbole, V. P.; Rohatgi, V. K.; Das, A. K.; Bhoraskar, S. Synthesis of Nanowires and Nanoparticles of Cubic Aluminium Nitride. *Nanotechnology* **2004**, *15*, 370–373.
26. Balasubramanian, C.; Bellucci, S.; Castrucci, P.; Crescenzi, M. D.; Bhoraskar, S. V. Scanning Tunneling Microscopy Observation of Coiled Aluminum Nitride Nanotubes. *Chem. Phys. Lett.* **2004**, *383*, 188–191.
27. Costales, A.; Blanco, M. A.; Francisco, E.; Pandey, R.; Pendas, A. M. Evolution of the Properties of Al_nN_n Clusters with Size. *J. Phys. Chem. B* **2005**, *109*, 24352–24360.
28. Zhang, D.; Zhang, R. Q. Geometrical Structures and Electronic Properties of AlN Fullerenes: A Comparative Theoretical Study of AlN Fullerenes with BN and C Fullerenes. *J. Mater. Chem.* **2005**, *15*, 3034–3038.
29. Li, J. L.; Xia, Y. Y.; Zhao, M. W.; Liu, X. D.; Song, C.; Li, L. J.; Li, F.; Huang, B. D. Theoretical Prediction for the $(AlN)_{12}$ Fullerene-Like Cage-Based Nanomaterials. *J. Phys.: Condens. Matter* **2007**, *19*, 346228-1–346228-8.
30. Wippermann, S.; Schmidt, W. G. Water Adsorption on Clean Ni(111) and p(2 × 2)-Ni(111)-O Surfaces Calculated from First Principles. *Phys. Rev. B* **2008**, *78*, 235439-1–235439-7.
31. Perdew, J. P.; Burke, K.; Ernzerhof, M. Generalized Gradient Approximation Made Simple. *Phys. Rev. Lett.* **1996**, *77*, 3865–3868.
32. Kresse, G.; Joubert, D. From Ultrasoft Pseudopotentials to the Projector Augmented-Wave Method. *Phys. Rev. B* **1999**, *59*, 1758–1775.
33. Kresse, G.; Furthmüller, J. Efficient Iterative Schemes for *Ab Initio* Total-Energy Calculations Using a Plane-Wave Basis Set. *Phys. Rev. B* **1996**, *54*, 11169–11186.
34. Wang, Y.; Perdew, J. P. Correlation Hole of the Spin-Polarized Electron-Gas, with Exact Small-Wave-Vector and High-Density Scaling. *Phys. Rev. B* **1991**, *44*, 13298–13307.
35. Monkhorst, H. J.; Pack, J. D. Special Points for Brillouin-Zone Integrations. *Phys. Rev. B* **1976**, *13*, 5188–5192.
36. Sun, Q.; Wang, Q.; Jena, P.; Reddy, B. V.; Marquez, M. Hydrogen Storage in Organometallic Structures Grafted on Silsesquioxanes. *Chem. Mater.* **2007**, *19*, 3074–3078.